AIMS Materials Science, 5(4): 614–623.
DOI: 10.3934/matersci.2018.4.614
Received: 08 May 2018
Accepted: 17 July 2018
Published: 26 July 2018

http://www.aimspress.com/journal/Materials

Research article

Effects of particle size of aluminum powder in silver/aluminum paste on n-type solar cells

Takayuki Aoyama[1,*], Mari Aoki[2], Isao Sumita[2] and Atsushi Ogura[3]

[1] Noritake Co., Limited, 300, Higashiyama, Miyoshi-Cho, Miyoshi, Aichi, 470-0293, Japan
[2] Asada Mesh Co., Ltd., 23-7, Shindo-4, Matsubara, Osaka, 580-0015, Japan
[3] Meiji University, 1-1-1, Higashi-Mita, Tana-Ku, Kawasaki, Kanagawa, 214-8571, Japan

* **Correspondence:** Email: takayuki_aoyama@n.noritake.co.jp; Tel: +81561766805; Fax: +81561344997.

Abstract: Silver paste, which mainly consists of silver metal, glass frit, and organics, has been used for contacting n^+ emitter of conventional p-type solar cells, whereas aluminum-added silver paste (silver/aluminum paste) has been used for p^+ emitter of n-type solar cells. It has been reported that the addition of aluminum powder to the silver paste decreases contact resistance between the paste electrodes and the p^+ emitter with increasing content of the aluminum powder in the paste, and in addition, that the silver/aluminum paste creates large and deep metallic spikes underneath the paste, which has been considered to decrease the contact resistance. However, how particle size of the aluminum powder affects the contact resistance and the electrical characteristics of the n-type solar cells has not been clear yet. In this study, the effects of the particle size of aluminum powder in the silver/aluminum paste on the contact resistance and the electrical characteristics are investigated. Our study demonstrates that the particle size of the aluminum powder strongly affects the contact resistance and the electrical characteristics. The contact resistance decreases not only with increasing the content of the aluminum powder in the silver/aluminum paste, but also with increasing the particle size of the powder. In addition, the optimization of the particle size of the aluminum powder can effectively increase *FF* of the n-type solar cells, resulting in increasing efficiency of the cells.

Keywords: silver/aluminum paste; n-type; solar cells; aluminum powder

1. Introduction

Conductive paste has held a prominent position on manufacturing silicon solar cells. Silver paste, which mainly consists of silver metal, glass frit, and organics, has been used for contacting the n^+ emitter of conventional p-type solar cells [1], whereas aluminum-added silver paste (silver/aluminum paste) has been applied for p^+ emitter of n-type solar cells [2]. The typical silver paste normally cannot contact p-type silicon with low contact resistance [2], but adding aluminum to the silver paste can effectively decrease the contact resistance [2]. The silver/aluminum contact has been applied to back side soldering pads for the conventional p-type solar cells to improve solderability of aluminum contact [3], but the aluminum in the silver/aluminum contact has been said to make electrical contact to p-type silicon [4]. Thus, the silver/aluminum paste is usually used as the contact for the p^+ emitter of the n-type solar cells.

The contact resistance of the silver/aluminum paste to the p^+ emitter decreases with increasing the content of the aluminum powder in the paste [2]. In addition, the silver/aluminum paste has been reported to create large and deep metallic spikes underneath the paste [5,6], which has been considered to play a role in the decrease of the contact resistance of the paste [5], because the number of the metallic spikes increases with increasing the aluminum content in the paste [7]. Meanwhile, it has been recently demonstrated that the special aluminum-free silver paste can electrically contact to p^+ emitter with low contact resistance [8], in which the metallic spikes are considered to cause shunts and recombination in the n-type solar cells. For these cases, the metallic spikes can play a big role for reducing the contact resistance, but in some cases the spikes might cause shunting of p-n junction and also severe recombination of free carriers to reduce the conversion efficiency [6]. However, our previous study has showed that the metallic spikes are not main reasons for the shunts and recombination, and that the silver/aluminum paste might have possibility to improve the quality of the contact even if the metallic spikes would be there [9]. In addition, how particle size of the aluminum powder affects the contact resistance and the electrical characteristics of the n-type solar cells has not been clear yet. For this reason, the effects of the particle size of the aluminum powder in the silver/aluminum paste on the contact resistance and the electrical characteristics must be clarified. In this study, the effects of the particle size of the aluminum powder in the silver/aluminum paste on the contact resistance and the electrical characteristics of the n-type solar cells are investigated. Our study will demonstrate that larger particle size of aluminum powder can effectively decrease the contact resistance of the silver/aluminum paste to the p^+ emitter, which increases the efficiency of the n-type solar cells.

2. Materials and method

2.1. Fabrication of n-type solar cells

The n-type solar cells were prepared to measure the contact resistance and the electrical characteristics. The n-type solar cells were made using n-type Cz-silicon wafers (156 mm × 156 mm), on both sides of which the surfaces were textured with a random pyramid structure. The sheet resistance of the boron-doped p^+ emitter and the phosphorus-doped n^+ back surface field (BSF) were approximately 70 Ω/□ and 40 Ω/□, respectively. The p^+ emitter and the n^+ BSF are both passivated by a SiO_2 and SiN_x stack layer. The SiO_2 layer was formed by thermal oxidation, and the SiN_x layer

was deposited with a plasma-enhanced chemical vapor deposition (PECVD). For the measurement of the contact resistance, homemade silver/aluminum pastes were screen-printed on the p^+ emitter side in the line pattern of the transfer length method (TLM) geometry shown in Figure 1 by using a screen printer, and dried at 120 ℃ for 10 minutes. The line length of the TLM pattern is 2 cm, and the distance of the adjacent lines are varied as 100, 300, 500, 800, 1200, 1500, 1800, and 2000 μm. After screen-printing and drying, the screen-printed pastes were fired with an infrared belt furnace at a set peak firing temperature of 910 ℃. Meanwhile, for the measurement of the electrical characteristics, the silver/aluminum pastes and commercially available silver paste were screen-printed on the p^+ emitter side and on the n^+ BSF side with a standard H-pattern consisted of 3 busbars and 80 fingers, respectively, as shown in Figure 2. After screen-printing and drying, the screen-printed pastes were co-fired with the same furnace. The illuminated *I–V* curves were measured with an *I–V* tester and a solar simulator under an air mass 1.5 G spectrum with an intensity of 100 mW/cm^2 at 25 ℃.

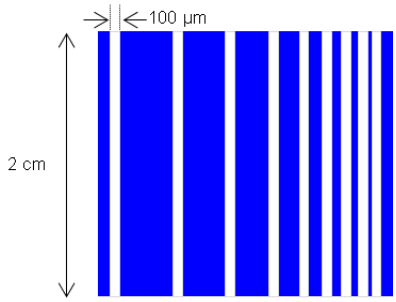

Figure 1. TLM line pattern used in this study. The gridlines whose length is 2 cm are separated with different spaces: 100, 300, 500, 800, 1200, 1500, 1800, and 2000 μm.

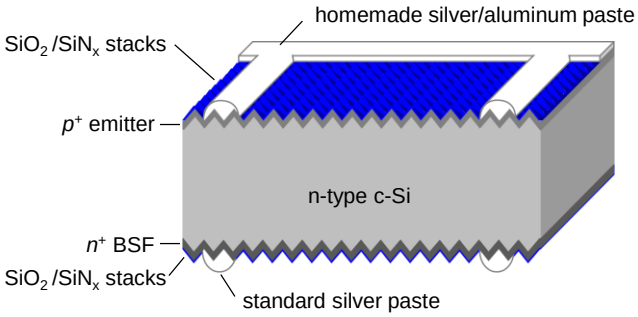

Figure 2. Structure of the n-type solar cell used in this study. The H-pattern gridlines of the n-type solar cells consist of 3 busbars and 80 fingers.

2.2. Constituents in silver/aluminum paste

The silver/aluminum pastes used in the study consists of silver powder, glass frit, organics, and aluminum powder. The glass frit mainly consists of silicon oxide, lead oxide, boron oxide, and zinc oxide. In this study, the particle size (particle diameter) and the content of the aluminum powder in the silver/aluminum pastes were varied, whereas the other constituents in the paste, i.e., the silver powder, the glass frit, and the organics, remained constant. For the particle size, three types of

aluminum powder with different particle-size distribution were prepared, whose particle diameters: D_{10}, D_{50}, and D_{90} are shown in Table 1. D_{10}, D_{50}, and D_{90} represent particle diameters at which 10, 50, and 90 volume percent of particles in a powder is comprised of less than these diameters; for example, in the case of the aluminum powder AP1S, 10 volume percent of the aluminum particles in the powder has the diameter less than 0.9 μm. In addition, SEM images of the three aluminum powders are shown in Figure 3. The aluminum content was defined as weight percent ratio of the aluminum powder to the silver in the paste, which were varied as "low", "middle", and "high" content in the range of below a few weigh percent.

Table 1. Particle size distribution of the aluminum powders used in this study.

Aluminum powder	D_{10}	D_{50}	D_{90}
AP1S	0.9 μm	1.7 μm	3.1 μm
AP2S	2.1 μm	4.4 μm	8.7 μm
AP3S	3.0 μm	7.3 μm	13.9 μm

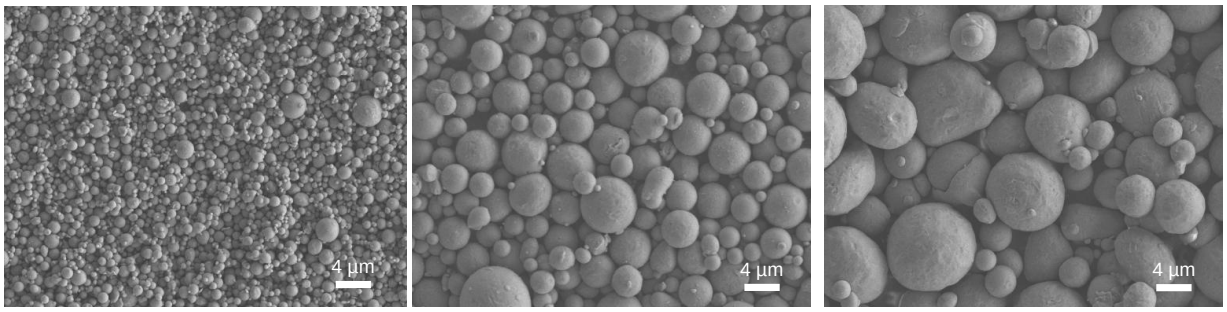

Figure 3. SEM images of the aluminum powders whose D_{50} values are (a) 1.7 μm, (b) 4.4 μm, and (c) 7.3 μm.

2.3. Observation of interface morphology

The interface morphology between the paste and the p^+ emitter was observed with a scanning electron microscope (SEM) after removal of the fired paste. For the observation, the bulk contact only was removed by a mixture of HNO_3 and HCl. The glass layer under the bulk contact was etched off by a diluted HF, and then metal precipitates under the glass layer were also etched off by the same mixed acid used in the removal of the bulk contact.

3. Results

3.1. Effects of aluminum powder on contact resistance

Figure 4 shows the dependence of the specific contact resistance ρ_c on the D_{50} of the aluminum powder in the silver/aluminum paste. It should be noted that the ρ_c of the silver paste with no aluminum was around 100 mΩcm^2, which was not plotted on Figure 4. For all the aluminum content

in the paste, the ρ_c monotonically decreases with increasing the D_{50} of the aluminum powder. In addition, a similar tendency can be observed in the dependence of the aluminum content in the paste on the ρ_c; specifically, the ρ_c decreases with increasing the aluminum content in the paste. The results clearly show that the larger particle size of the aluminum powder can effectively reduce the contact resistance of the silver/aluminum paste to the p^+ emitter. For instance, the ρ_c for the high content of the aluminum powder with the D_{50}: 1.7 μm is approximately 50 mΩcm^2, whereas that for the same content of the powder with the D_{50}: 7.3 μm is approximately 1 mΩcm^2.

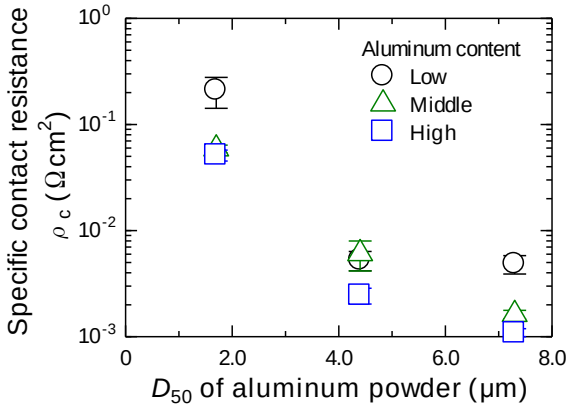

Figure 4. Dependence of the ρ_c on the content of the aluminum powder in the silver/aluminum paste. The larger particle size of the aluminum powder can effectively reduce the contact resistance of the silver/aluminum paste to the p^+ emitter.

3.2. Effects of aluminum powder on electrical characteristics of n-type solar cells

Subsequently, the effects of the particle size of the aluminum powder on the electrical characteristics of the n-type solar cells are investigated. Figure 5 shows dependence of the cell parameters, *FF*, V_{oc}, J_{sc}, *Eff.*, on the D_{50} of the aluminum powder in the paste. The *FF* of the n-type solar cells increases with increasing the D_{50} of the aluminum powder and with increasing the aluminum content in the paste. By contrast, dependence of the V_{oc} on the D_{50} of the aluminum powder is different depending on the aluminum content in the paste. For the low and middle aluminum content, the V_{oc} decreases with increasing the D_{50} of the aluminum powder. On the other hand, the V_{oc} of the high aluminum content increases with increasing the D_{50}, but the V_{oc} gets to the same value, i.e., around 633 mV, regardless of the aluminum content. In addition, the dependence of the V_{oc} on the aluminum content in the paste becomes weaker as increasing the D_{50}. Meanwhile, the J_{sc} of the solar cells slightly increases with increasing the D_{50} of the aluminum powder. Hence, the efficiency of the n-type solar cells increases with increasing the D_{50} of the aluminum powder, which correlates well with the dependence of the *FF* on the D_{50}; then, the n-type solar cells with the silver/aluminum paste using the aluminum powder of D_{50}: 7.3 μm can effectively increase the efficiency of the cells.

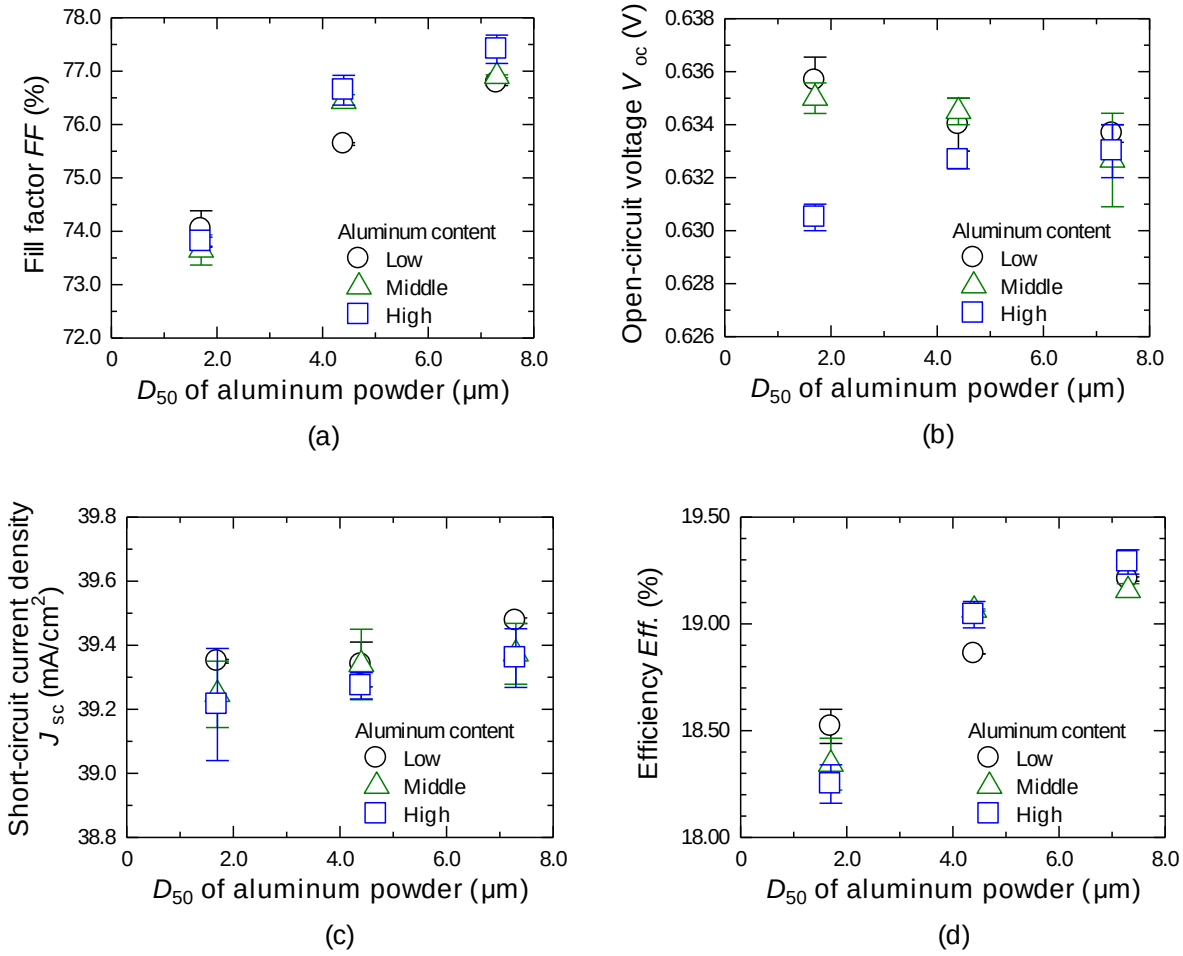

Figure 5. Dependence of the cell parameters: (a) fill factor *FF*, (b) open-circuit voltage V_{oc}, (c) short-circuit current J_{sc}, and (d) efficiency *Eff.*, on the particle size of the aluminum powder in the silver/aluminum paste. The *FF* of the n-type solar cells increases with increasing the D_{50} of the aluminum powder and with increasing the aluminum content in the paste. By contrast, the dependence of the V_{oc} on the D_{50} of the aluminum powder is different depending on the aluminum content in the paste. For the low and middle aluminum content, the V_{oc} decreases with increasing the D_{50} of the aluminum powder. On the other hand, the V_{oc} using the pastes with the high aluminum content increases with increasing the D_{50}, but the V_{oc} gets to the same value, i.e., around 633 mV, regardless of the aluminum content.

3.3. Interface morphology underneath silver/aluminum paste

Figures 6 and 7 show the interface morphology underneath the silver paste with no aluminum and the silver/aluminum paste with the high content of aluminum powder. Top-views of the interface morphology after the removal of the bulk contact and the underlying glass layer are shown in Figure 6. Metal precipitates appear on the silicon surface after the removal. Actually, many precipitates, which are silver crystallites precipitated from the silver paste with no aluminum during the firing, are observed underneath the paste, as shown in Figure 6a. By contrast, the silver crystallites become

smaller by adding aluminum to the paste, and in addition large pits can be observed underneath all silver/aluminum pastes.

Figure 7 shows top-views of the interface morphology after the removal of the metal precipitates by the mixed acid. The morphology of the wafer surface deformed by the pastes can be observed by the removal of the metal precipitates. Actually, the morphology deformed by the silver paste and the silver/aluminum pastes can be clearly seen in Figure 7. Many pits which are imprints of the silver crystallites can be observed underneath the silver paste with no aluminum, but the silver crystallite imprints become smaller by adding the aluminum to the paste. The imprints underneath the silver/aluminum paste with the aluminum powder of D_{50}: 1.7 μm are obviously smaller compared with that underneath the silver paste. On the other hand, the silver crystallite imprints become fewer with increasing the D_{50} of the aluminum powder; instead, large pits whose sizes are comparable with the texture can be observed underneath the silver/aluminum paste. In addition, the large pits increase with increasing the D_{50} of the aluminum powder. It has been reported that the large pits are formed by metallic spikes due to aluminum addition to silver paste. Thus, the large pits observed in this study are obviously caused by the aluminum addition.

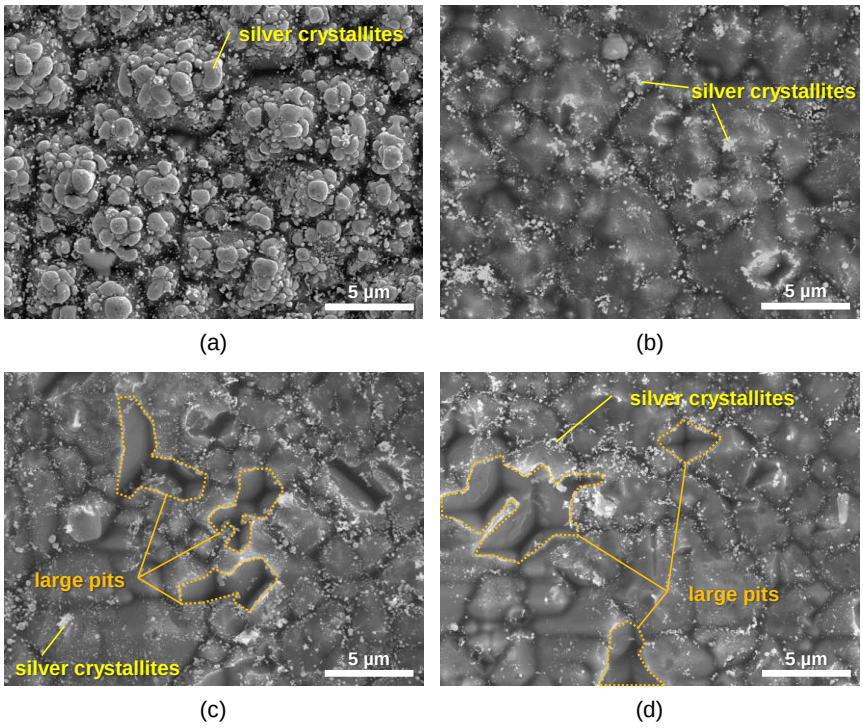

Figure 6. Top-view SEM images of the interface morphology underneath (a) the silver paste with no aluminum and the silver/aluminum pastes with high aluminum content, in which the D_{50} of the aluminum powder is: (b) 1.7 μm, (c) 4.4 μm, and (d) 7.3 μm after the bulk silver and the underlying glass layer were removed. Many silver crystallites are observed underneath the silver paste with no aluminum, but the crystallites become fewer and smaller by adding aluminum to the paste, instead huge pits can be observed underneath all silver/aluminum pastes.

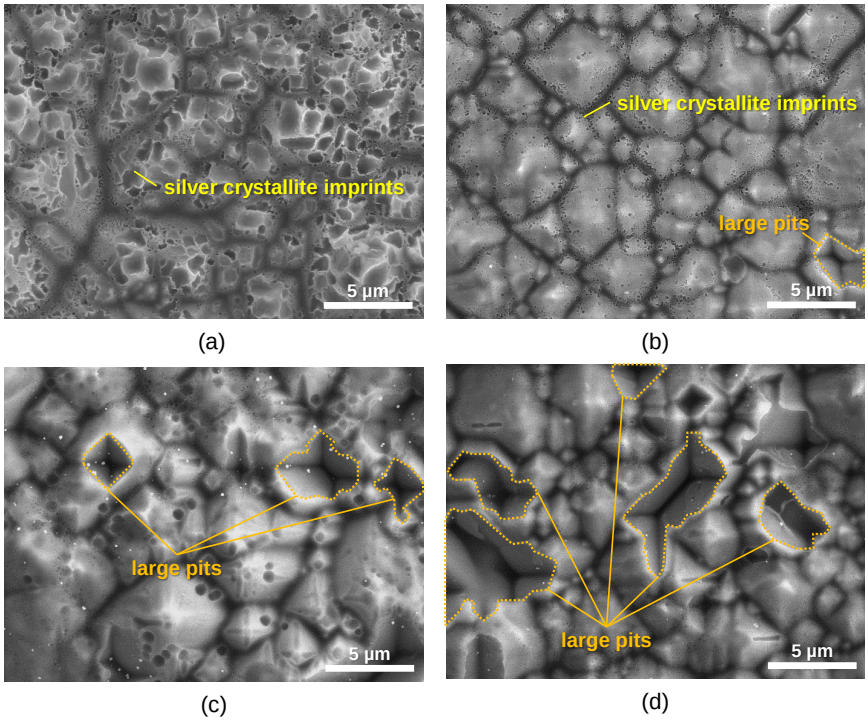

Figure 7. Top-view SEM images underneath (a) the silver paste with no aluminum and the silver/aluminum paste with high aluminum powder content whose D_{50} is: (b) 1.7 μm, (c) 4.4 μm, and (d) 7.3 μm after removal of the metal precipitates. Many pits which are imprints of the silver crystallites can be observed underneath the silver paste with no aluminum, but the silver crystallite imprints become smaller by adding the aluminum to the paste. In addition, the imprints become fewer with increasing the D_{50} of the aluminum powder in the silver/aluminum paste, instead the large pits can be observed underneath the all silver/aluminum pastes.

4. Discussion

In this study, the effects of the particle size of the aluminum powder in the silver/aluminum paste on the contact resistance and the electrical characteristics of the n-type solar cells are investigated. The contact resistance of the silver/aluminum paste decreases with increasing the aluminum content in the silver/aluminum paste, which is consistent with the results of previous researchers [2], but it was also demonstrated that the contact resistance decreases with increasing the particle size of the aluminum powder. Since the surface of the aluminum particle is oxidized [10], the metal aluminum in the particle needs to burst through the external oxide layer during the firing to affect the contact formation between the silver/aluminum paste and the p^+ emitter [7]. In addition, the volume ratio of the metal aluminum to the full volume of the aluminum particle increases with increasing the aluminum particle size. Hence, the larger the aluminum particle size becomes, the easier the metal aluminum in the aluminum particle can burst through the external oxide layer; therefore, the contact resistance decreases with increasing the particle size of the aluminum powder. In addition, the size of the large pits increases with increasing the particle size of the aluminum powder, which correlates with the dependence of the contact resistance on the particle size of the

aluminum powder; therefore, the large metallic spikes must relate to the contact resistance decrease. In addition, the interface morphology indicates that the silver crystallites do not have the predominant effect on the contact resistance decrease, because the contact resistance decreases with increasing the aluminum content though the number of the crystallites decreases.

The dependence of the contact resistance on the aluminum powder in the silver/aluminum paste strongly correlates with the dependence of the *FF* on the aluminum powder; that is, the *FF* increases with increasing the particle size of the aluminum powder and with increasing the aluminum content in the paste. Thus, the *FF* increase can be explained by the contact resistance decrease due to the particle size of the aluminum powder and the aluminum content in the paste. In contrast, the dependence of the V_{oc} on the particle size of the aluminum powder is different depending on the aluminum content in the silver/aluminum paste. For the low and middle aluminum content, the V_{oc} decreases with the particle size increase of the aluminum powder, whereas for the high aluminum content in the paste the V_{oc} slightly increases. Then, the larger particle size of the aluminum powder in the silver/aluminum paste can effectively decrease the contact resistance, which can increase the *FF*, resulting in increasing the efficiency of the n-type solar cells.

5. Conclusions

In this study, the effects of the particle size of the aluminum powder in the silver/aluminum paste on the contact resistance and the electrical characteristics of the n-type solar cells are investigated. Our study demonstrates that the contact resistance decreases not only with increasing the aluminum content in the paste, but also with increasing the particle size of the aluminum powder.

The contact resistance decrease by the aluminum addition can relate to the large metallic spikes underneath the silver/aluminum paste. The dependence of the *FF* of the solar cells on the particle size of the aluminum powder correlates well with that of the contact resistance on the particle size. Thus, the aluminum powder with the large particle size can effectively reduce the contact resistance of the paste. By contrast, the V_{oc} of the silver/aluminum paste with such a larger size of the aluminum powder is lower than that with the smaller size of the aluminum powder. Then, the n-type solar cells with the silver/aluminum paste containing larger particle size of the aluminum powder show the higher efficiency due to the higher *FF*. The cell efficiency, however, should further increase when the higher *FF* realized by the high aluminum content with the D_{50}: 7.3 μm and the higher V_{oc} realized by the low aluminum content with the D_{50}: 1.7 μm are simultaneously achieved.

Conflict of interest

The authors declare no conflicts of interest associated with the study.

References

1. Lin HC, Spittlehouse DP, Hsueh YW (1978) Contact resistance of silver ink on solar cell. *13th Photovoltaic Specialists Conference*, Washington, DC, USA, 593–596.
2. Kerp H, Kim S, Lago R, et al. (2006) Development of screen printable contacts for p^+ emitters in bifacial solar cells. *21st European Photovoltaic Solar Energy Conference*, Dresden, Germany, 892–894.

3. Field MB, Scudder LR (1976) Application of thick-film technology to solar cell fabrication. *12th Photovoltaic Specialists Conference*, Baton Rouge, Louisiana, USA, 303–308.
4. Mandelkorn J, Lamneck JH (1975) Advances in the theory and application of BSF cells. *11th Photovoltaic Specialists Conference*, Scottsdale, Arizona, USA, 36–39.
5. Riegel S, Mutter F, Hahn G, et al. (2010) Contact formation in the silver/aluminum thick film firing process: A phenomenological approach. *25th European Photovoltaic Solar Energy Conference and Exhibition*, Valencia, Spain, 2353–2356.
6. Lago R, Pérez L, Kerp H, et al. (2010) Screen printing metallization of boron emitters. *Prog Photovoltaics* 18: 20–27.
7. Fritz S, König M, Riegel S, et al. (2015) Formation of Ag/Al screen-printing contacts on B emitters. *IEEE J Photovolt* 5: 145–151.
8. Fritz S, Engelhardt J, Ebert S, et al. (2016) Contacting boron emitters on n-type silicon solar cells with aluminium-free silver screen-printing pastes. *Phys Status Solidi-R* 10: 305–309.
9. Aoyama T, Aoki M, Sumita I, et al. (2016) Effects of aluminum in metallization paste on the electrical losses in bifacial n-type crystalline silicon solar cells. *Energy Procedia* 98: 106–114.
10. Wefers K, Misra C (1987) Oxides and Hydroxides of Aluminum. Alcoa Technical Paper No. 19, Revised, Alcoa Laboratories.